 doi:10.20944/preprints202109.0424.v1

Article

Microfluidic Lab-On-a-Chip based on UHF-Dielectrophoresis for Stemness Phenotype Characterization and Discrimination among Glioblastoma Cells

Elisa Lambert[1,†], Rémi Manczak[1,†], Elodie Barthout[2,†], Sofiane Saada[2], Elena Porcù[3,4], Francesca Maule[5], Barbara Bessette[2], Giampietro Viola[3,4], Luca Persano[3,4], Claire Dalmay[1,†], Fabrice Lalloué[2,†], Arnaud Pothier[1,†,*]

[1] XLIM-UMR 7252, University of Limoges/CNRS, 87060 Limoges, France; remi.manczak@xlim.fr (R.M.); claire.dalmay@xlim.fr (C.D.); elisa.lambert@xlim.fr (E.L.)
[2] CAPTuR-EA 3842, University of Limoges, 87025 Limoges, France; elodie.barthout@unilim.fr (E.B.); sofiane.saada@unilim.fr (S.S.); barbara.bessette@unilim.fr (B.B.); fabrice.lalloue@unilim.fr (F.L.)
[3] Department of Women's and Children's Health (DSB), University of Padova, 35128 Padova, Italy; elena.porcu@gmail.com (E.P.); luca.persano@unipd.it (L.P.); giampietro.viola.1@unipd.it (G.V.)
[4] Institute of Pediatric Research (IRP), 35127 Padova, Italy
[5] Arnie Charbonneau Cancer Institute, Department of Biochemistry and Molecular Biology, University of Calgary, Calgary, Canada; francesca.maule@ucalgary.ca (F.M.)
† These authors contributed equally to this work
* Correspondence: arnaud.pothier@xlim.fr (A.P.)

Abstract: Glioblastoma (GBM) is one of the most aggressive solid tumors, particularly due to the presence of cancer stem cells (CSCs). Today the characterization of this type of cells with an efficient, fast and low-cost method remains an issue. Hence, we have developed a microfluidic lab-on-a-chip based on dielectrophoresis (DEP) single cell electro-manipulation to measure the two crossover frequencies: f_{x01} in low frequency range (below 500 kHz) and f_{x02} in Ultra High Frequency range (UHF, above 50 MHz). First, *in vitro* conditions were investigated. U87-MG cell lines were cultured in different conditions in order to induce an undifferentiated phenotype. Then, *ex vivo* GBM cells from patients' primary cell culture, were passed through the developed microfluidic system and characterized in order to reflect clinical conditions. This article demonstrates that the usual exploitation of low frequency range DEP does not allow the discrimination of the undifferentiated from the differentiated phenotypes of GBM cells. However, the presented study highlights the use of UHF-DEP as a relevant discriminant parameter. The proposed microfluidic lab-on-a-chip is able to follow the kinetic of U87-MG phenotype transformation in a CSC enrichment medium and their cancer stem cells phenotype acquirement.

Keywords: high frequency dielectrophoresis; glioblastoma cells; single cell manipulation; microfluidic point-of-care device; cancer stem cells

1. Introduction

Glioblastoma (GBM) is the most frequent and highly malignant brain tumor in adulthood classified as a high-grade glioma (grade IV). Thus, it is one of the most aggressive tumors of the central nervous system. Worldwide, 240,000 brain tumors are diagnosed each year, the majority of which are GBM [1]. GBM is associated with a poor prognosis with a mean survival of 12 months. Indeed, standard treatment such as surgery and combined radio-chemotherapy fails to improve patients management [2]. Despite recent advances in targeting therapies and immunotherapy, the current treatment does not allow the improvement of the patient survival statistics. This very poor prognosis is mainly due to a frequent relapse despite the regression or disappearance of the tumor upon the golden standard treatment, i.e. Stupp protocol [3]. Consequently, this pathology is very difficult to handle.

Preprints (www.preprints.org) | NOT PEER-REVIEWED | Posted: 24 September 2021 doi:10.20944/preprints202109.0424.v1

The high recurrence of GBM can be explained by the high cellular, genetic and morphological heterogeneity of the tumor cell population present in the tumor [4], which alters the efficiency of conventional therapies. Especially, a small cell sub-population, called cancer stem cells (CSCs) plays a major role in this recurrence [4]. They display an immature and undifferentiated phenotype and have specific self-renewal features. They also are likely to regenerate tumor. Moreover, as chemotherapy targets cells that divide very rapidly, CSCs escape this current treatment due to their quiescent properties [1]. The presence of these cells in solid tumor is a cue of tumor aggressiveness; hence, the identification and detection of this rare cell subpopulation inside tumor is crucial.

In this objective, biologists currently analyze a panel of biomarkers (protein and nucleic) by using conventional approaches for characterizing CSCs such as immunofluorescence, flow cytometry, Real-time qPCR and protein array analysis. These tools require labelling to identify CSCs, thereby present several drawbacks (expensive equipment and time-consuming). In addition, immunolabeling can influence cell behavior and differentiation mechanism, limits further analyses and may interfere with the cell culture [5]. In order to overcome these issues, researchers started to develop alternative label-free methods for cell characterization. These innovative technics most often rely on an external force coupled with microfluidics. It allows the reduction of the cost and analysis time with the possibility of parallelization and the reduction of sample volume as only few µL are needed. It prevents also cells from damages by limiting mechanical constraints. Among the label-free method, dielectrophoresis (DEP) presents an important interest as it allows the investigation of biological cell behavior according to its intrinsic dielectric properties. For this study, we use DEP electro-manipulation at low frequency (below 500 kHz) and at Ultra High Frequency (UHF) range (above 50 MHz), in order to highlight the relevance of using UHF-DEP phenomenon to discriminate undifferentiated cells (CSC) from differentiated tumor cells. Implementation of the proposed microfluidic lab-on-a-chip is done on BiCMOS technology and allows the screening of the intracellular properties of GBM cells.

1.1. Basic DEP theory

Dielectrophoresis is a physical phenomenon, which leads to the motion of a polarizable particle such as biological cells, in a non-uniform electric field due to the interaction between the induced dipole of the particle and the field gradient. The polarization phenomenon redistributes of the charges at the interface between the particle and the suspension medium. The dielectrophoretic force exerted on the polarized particle in a non-uniform electric field is expressed as follows [6]:

$$F_{DEP} = 2\pi r^3 \varepsilon_m \mathrm{Re}[f_{CM}(\omega)] \nabla E^2 \quad (1)$$

where r is the radius of the particle, ε_m the permittivity of the suspension medium, $\mathrm{Re}[f_{CM}(\omega)]$ the real part of the Clausius-Mossotti (CM) factor, E the applied electric field.

The Clausius-Mossotti factor describes the polarization state of a particle in a suspension medium. It depends of the dielectric properties (permittivity and conductivity) of the medium and the particle [6]:

$$f_{CM}(\omega) = \frac{\varepsilon_p^* - \varepsilon_m^*}{\varepsilon_p^* + 2\varepsilon_m^*} \quad (2)$$

where ε_p^* and ε_m^* are the complex permittivity of the particle and the medium respectively. The complex permittivity can be defined as:

$$\varepsilon^* = \varepsilon - j\frac{\sigma}{\omega} \quad (3)$$

where ε is the permittivity, σ the conductivity and ω the angular frequency of the electric field. The sign of the real part of the CM factor determines the orientation of the DEP force. In Figure 1a, when $\mathrm{Re}[f_{CM}(\omega)]$ is positive, the DEP force attracts the particle to the strong

Preprints (www.preprints.org) | NOT PEER-REVIEWED | Posted: 24 September 2021 doi:10.20944/preprints202109.0424.v1

field areas. This phenomenon is called positive DEP (pDEP). In Figure 1b, when Re[$f_{CM}(\omega)$] is negative, the DEP force is then repulsive and the particle is repelled towards the weak electric field areas. It is so-called negative DEP (nDEP).

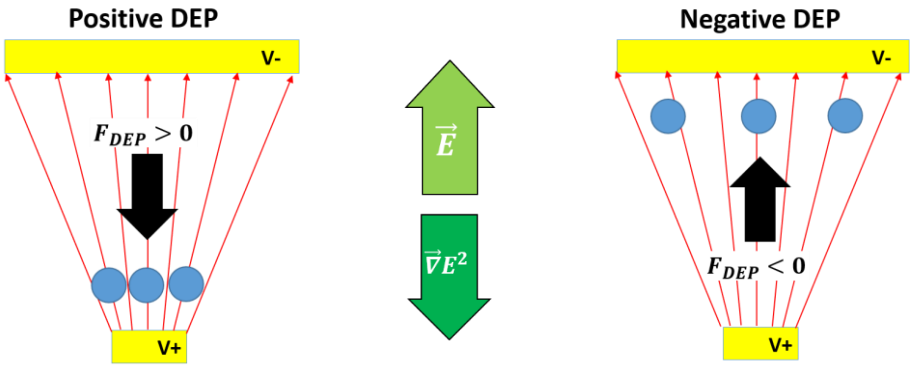

(**a**) (**b**)

Figure 1. Particles interaction in a non-uniform applied field: (**a**) the DEP force is positive, i.e. collinear to the electric field gradient ∇E^2, and the particles are attracted to areas of high field intensity (positive DEP); (**b**) the DEP force is negative, i.e. opposite to the electric field gradient ∇E^2, and the particles are repelled toward areas of low field intensity (negative DEP).

From a physic point of view, a biological cell can be modelized as a spherical dielectric particle that is submitted to the DEP force. A cell is a complex biological object, but it can be properly modeled into a simpler single-shell model with a reduced number of dielectric parameters associated to each component of the cell.

1.2. From a biological cell to a single-shell model

In order to predict cell's behavior with an applied electric field, it is helpful to have a simplified model of a biological cell. The Figure 2 presents a schematic of a cell and its commonly used associated single-shell model associated where the cell membrane and cytoplasm are representing by a shell and a core with their own complex permittivity [7–9].

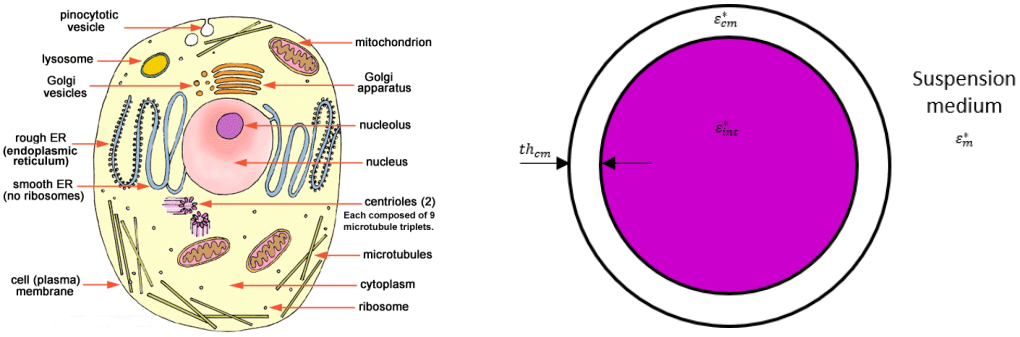

(**a**) (**b**)

Figure 2. (**a**) Representation of a biological cell in a suspension medium; (**b**) its single-shell model with ε^*_{int} the complex permittivity of the cellular content, ε^*_{cm} the complex permittivity of the cell membrane and th_{cm} the thickness of the cell membrane and ε^*_m the complex permittivity of the suspension medium.

Indeed, the single-shell model considers the cytoplasm and its content as a homogeneous dielectric sphere enveloped by the plasma membrane. This model limits the number of dielectric parameters to take into account only the complex permittivity of the intracellular content, the cell membrane and the suspension medium. Actually, the Clausius-Mossotti factor depends on these parameters as well as the frequency of the applied field. This single-shell model will be considered in this paper.

Preprints (www.preprints.org) | NOT PEER-REVIEWED | Posted: 24 September 2021 doi:10.20944/preprints202109.0424.v1

1.3. Effect of the cellular dielectric properties on the Clausius-Mossotti factor

Figure 3 illustrates the frequency-dependent cell behavior through the real part of the CM factor (Figure 3a). The dielectric parameters and cell geometric parameters are reported in Table 1. The real part plot in Figure 3a is computed thanks to the myDEP software [10]. nDEP behavior can be observed at very low frequency (lower than 400 kHz) and at high frequency (at least higher than 150 MHz), and pDEP behavior can be seen for medium range frequency (between 500 kHz and 100 MHz). The plot of the CM factor hence, presents alternations between repulsive state (nDEP) and attractive state (pDEP). Two crossover frequencies f_{x01} and f_{x02} appear where the real part of the CM factor becomes null. f_{x01} occurs at low frequency whereas f_{x02} occurs at higher frequency.

Moreover, from Figure 3a, 100 kHz, 1 MHz, 20 MHz and 500 MHz frequencies were selected in order to study the dielectric response of the cells. Indeed, these frequencies correspond to the two different DEP behaviors but at low frequency (frequencies n°1 and n°2) and at high frequency regime (frequencies n°3 and n°4). COMSOL Multiphysics® computations were done with the AC/DC electric current module in Figure 3b. The parameters from Table 1 were used for the simulation in such a way that the results correspond to the curve of the real part of the CM factor. As said before, the cell is represented by the single-shell model with the core: its intracellular content, and the shell: its plasma membrane. The cell is considered here to be suspended in a low conductivity medium. The electric potential is 1 Vpp. The shown colors represent the electric field intensity in V/m from dark blue (the field intensity is 0 V/m) to dark red (the field intensity is maximum). One can notice that for the nDEP behavior (at 100 kHz and 500 MHz), the electric field lines (black streamlines) bypass the cell whereas for the pDEP behavior (at 1 MHz and 20 MHz), the electric field lines seem attracted inside the cell. This is mainly due to the reorientation of the charges at the interface between the cell membrane and the medium [6]. One can also notice that at low frequency, no field can reach the cell content. The electric field is maximum inside the plasma membrane, which hence acts as an insulator. As a result, at low frequency, the electromagnetic field will be more sensitive to the physical and dielectric properties of the cell membrane. The more the frequency of the applied signal increases, the more the electric field can penetrate inside the cell and starts to interact with and so probe the cellular content. Consequently, at high frequency, the electromagnetic wave can deeply be sensitive to the intracellular content.

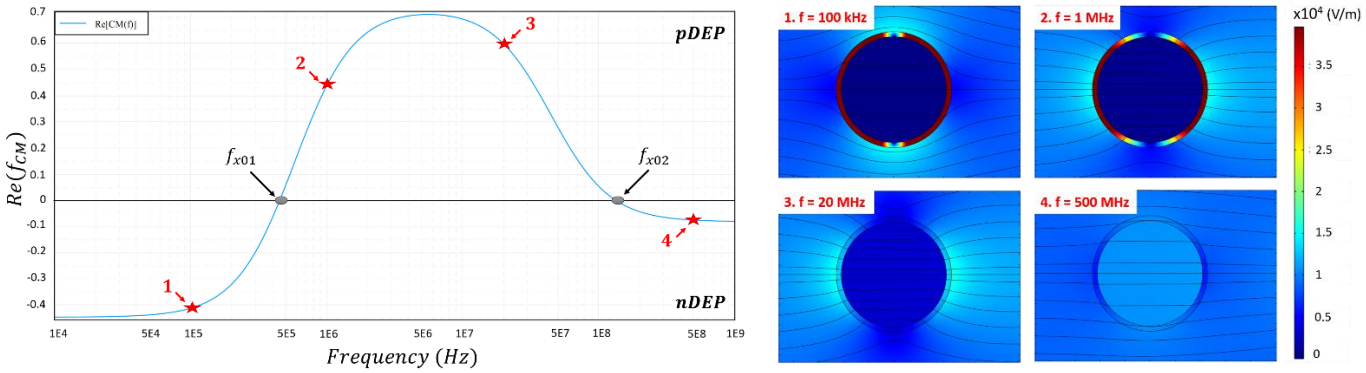

(**a**) (**b**)

Figure 3. Numerical simulation of a cell dielectric behavior in function of the frequency with the parameters from Table 1. The design used for the biological cell is the single-shell model. (**a**) Numerical simulation of the real part of the Clausius-Mossotti factor. The red stars correspond to the chosen frequencies for the COMSOL simulation; (**b**) COMSOL simulation of the single-shell model for different frequencies (100 kHz; 1 MHz; 20 MHz; 500 MHz) which correspond to the curve of

Preprints (www.preprints.org) | NOT PEER-REVIEWED | Posted: 24 September 2021 doi:10.20944/preprints202109.0424.v1

the CM factor. The color scale corresponds to the electric field intensity (V/m) and the black lines correspond to the electric streamlines.

Table 1. Values of the different dielectric and cellular parameters used in the COMSOL Multiphysics simulation.

Parameter	Value
Particle radius	11.5 µm
Membrane thickness	700 nm[1]
Intracellular relative permittivity	50
Intracellular conductivity	0.5 S/m
Membrane relative permittivity	100[2]
Membrane conductivity	1.43 e-4 S/m[2]
Medium relative permittivity	78
Medium conductivity	0.02 S/m

[1] Membrane thickness was increased by 100 in order to avoid mesh issues during the computation.
[2] Data were modified proportionally due the modification of the membrane thickness in order to respect the cell dielectric behavior.

Moreover, it is possible to change the value of the dielectric parameters in order to study the evolution of the real part of the CM factor and the parameter-dependency of the two crossover frequencies as it has been done in [11–13]. A first approximation of the crossover frequency f_{x01} can be expressed as [6]:

$$f_{x01} = \sigma_m \frac{th_{cm}}{\sqrt{2}\pi\, r\, \varepsilon_{cm}} \quad (4)$$

The crossover frequency f_{x01} depends mostly on the dielectric parameters of the plasma membrane but also the particle radius. Hence, f_{x01} is more sensitive to the cell shape, its morphology and to the plasma membrane properties. It has been wildly used to separate cells or polystyrene particles of different size [14,15] and to separate living from non-viable cells [16]. The second crossover frequency f_{x02} can be approximated with the assumption that the conductivity of the suspending medium (20 mS/m, see Material and Methods section) is significantly below the intracellular value expression [17]:

$$f_{x02} = \frac{\sigma_{int}}{2\pi} \sqrt{\frac{1}{2\varepsilon_m^2 - \varepsilon_{int}\varepsilon_m - \varepsilon_{int}^2}} \quad (5)$$

The crossover frequency f_{x02} depends on the dielectric parameters of the intracellular content [18]. Hence, cells can be individually electro-manipulated by the DEP force motion according to their own dielectric properties of their cytoplasm. As an example, UHF-DEP has already been successfully used in order to discriminate differentiated from undifferentiated medulloblastoma cells [19,20].

This paper aims to show the relevance of the identification of the crossover frequency f_{x02} as the DEP signature and then, using it as an appropriate discriminant biomarker to detect CSCs within tumor cell population. Therefore, the two crossover frequencies f_{x01} and f_{x02} have been measured for each investigated GBM cell and compared.

2. Materials and Methods

2.1. Cell line culture

Human GBM cell lines U87-MG were purchased from American Type Culture Collection (ATCC). Cells were grown in different culture conditions (see below) at 37°C in a humidified atmosphere of 5% CO_2 – 95% air. Cancer stem cells enrichment from cell sub-

 doi:10.20944/preprints202109.0424.v1

population were obtained submitting them to stringent culture conditions with the Define Medium (DM). Two culture conditions were used for the cells' DEP characterization:

- Normal Normoxia Medium (NM): induces normal differentiation conditions in DMEM medium supplemented by 10% FBS, 2 mM glutamine and 1% penicillin/streptomycin
- Define Normoxia Medium (DM): induces stringent conditions in selective DMEM/F12 supplemented by 0.6% glucose, 1% sodium bicarbonate, 1% MEM non-essential amino acids, 5 mM HEPES, 9.6 µg/mL putrescine, 10 µg/mL ITSS, 0.063 µg/mL progesterone, 60 µg/mL N-acetyl-L-cysteine, 2 µg/mL heparin, 0.1 mg/mL penicillin/streptomycin, 50X B-27 supplement without vitamin A, 20 ng/mL EGF, 20 ng/mL bFGF

Hence, it is expected that the defined medium will select undifferentiated cells and also promote the emergence of CSC whereas the normal medium will induce a differentiation of cells and so will result in a very low ratio of cancer stem cells. For the differentiated cells, they were cultured during 6 days in NM medium before the DEP characterization. For the undifferentiated cells, they were cultured during 5 days in DM medium or maintained during 21 days in DM medium in order to study the kinetics of CSC appearance and the emergence of stem cells characteristics.

2.2. Primary GBM cell isolations, culturing and separation by flow cytometry

For some validation experiments, four different primary cell cultures have been isolated and established in vitro from GBM patients in order to characterize any potential difference in term of DEP signature between bulk cells and their relative CSC counterparts. Written informed consent for the donation of adult tumor brain tissues was obtained from patients before tissue collection under the auspices of the protocol for the acquisition of human brain tissues obtained from the Ethical Committee of the Padova University-Hospital (2462P). In particular, GBM cells were isolated from tumors at surgery as previously described [21]. Briefly, resected GBM samples were dissociated, and single cell suspensions grown in Define Medium under hypoxic conditions (DH). Indeed, GBM cells were maintained in an atmosphere of 2% oxygen, 5% carbon dioxide and balanced nitrogen in a H35 hypoxic cabinet (Don Whitley Scientific Ltd, Shipley, UK) to achieve a proper expansion of the CSC subpopulation in hypoxic conditions mimicking the GBM microenvironment [22].

After proper expansion *in vitro*, primary GBM cells were incubated with a PE mouse anti-CD133 (AC133) antibody (Miltenyi Biotec, Bergisch Gladbach, DE) according to manufacturer's indications and then separated into a CD133+ and a CD133- subpopulation by means of Fluorescence Activated Cell Sorting (FACS) in a MoFlo XDP cell sorter (Beckman Coulter, Brea, CA). A CD133 versus side scatter dot plot revealed the populations of interest characterized by the expression (or not) of the CD133 marker. Cell fractions were selected by setting appropriate sorting gates as previously described [23]. Upon sorting, isolated GBM cell subpopulations (CD133+ and CD133-) were washed in Phosphate Buffered Saline (PBS), frozen in 10% DMSO containing medium and then cryopreserved in liquid nitrogen for subsequent thawing and DEP characterization.

2.3. DEP suspension medium

Few minutes from the DEP characterization, U87-MG cells were suspended in an osmotic medium adapted for DEP electro-manipulation made from deionized water (ion free) supplemented by sucrose. The conductivity of the DEP medium is 26 mS/m and the pH is 7.4. The crossover frequency measurements were performed at room temperature.

2.4. Comparative transcriptomic analysis (mRNA levels) of the stemness phenotype

In order to confirm the enrichment of undifferentiated cells in the define medium (DM), a comparative transcriptomic analysis of the stemness phenotype was performed.

Preprints (www.preprints.org) | NOT PEER-REVIEWED | Posted: 24 September 2021 doi:10.20944/preprints202109.0424.v1

The extraction of the total RNA from U87-MG cell line was carried out using the RNeasy kit (Qiagen) on 1 million cells according to the manufacturer's recommendations. Quantitative Polymerase Chain Reaction (qPCR) was performed on 50 ng of cDNA using Taqman probes on GAPDH and HPRT as reference genes. The CSC markers used are CD133, Nanog, Sox2 and Oct4. The analysis is performed using QuantStudio3 (Thermo Fisher) and relative expressions are estimated by ΔΔCt method using the average of the two reference genes as endogenous control.

2.5. Crossover frequency experiment

2.5.1. DEP sensor design and experimental setup

In order to identify the cells' DEP signature, we use a specific BiCMOS RF-sensor implemented on a microfluidic chip, as presented in Figure 4. The developed UHF-DEP lab-on-chip allows the electro-manipulation of one single cell. Its structure is made of four electrodes to generate a non-uniform electric field. They are set at 90° across the microfluidic channel. In order not to disturb the fluid flow and not to obstruct the channel with the passage of cells, the two electrodes parallel to the channel (in dark grey in Figure 4b) are very thin with 0.45 µm high. The other pair of electrodes perpendicular to the channel are thicker: 9 µm high; in order to ensure a sufficiently strong field over the height of the channel. The implemented gaps between the electrodes are 40 µm wide to generate dielectrophoretic force with a low applied voltage to trap efficiently biological cells. The two pairs of electrodes are biased with a high frequency continuous wave (CW) signal. The fabrication process of the chip is detailed in [24]. The microfluidic channel is molded in a polydimethylsiloxane (PDMS) cap to drive the cell suspension to the sensor array. The channel is 150 µm wide and 50 µm high.

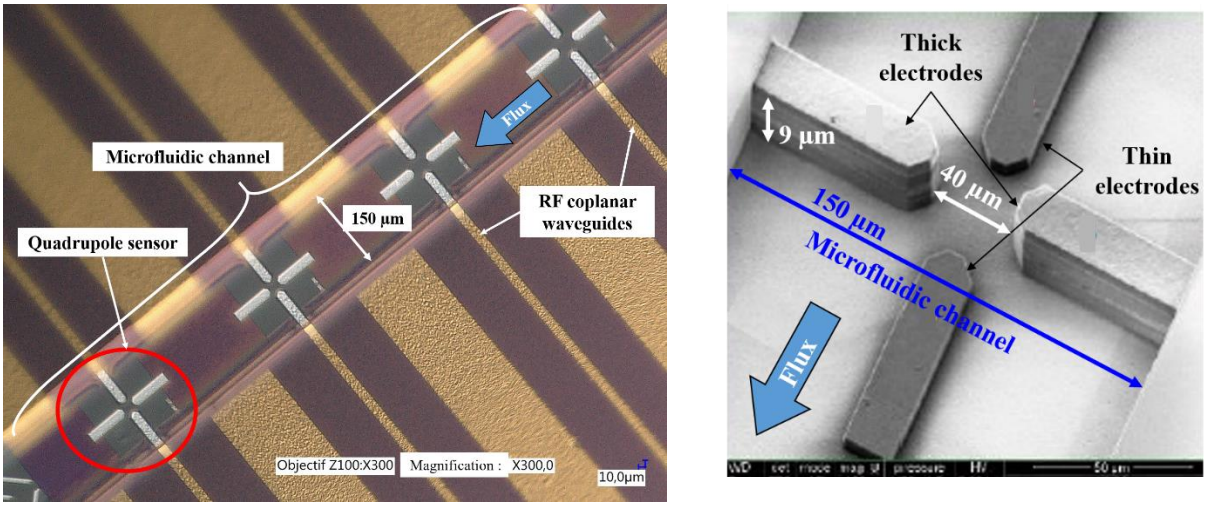

(**a**) (**b**)

Figure 4. (**a**) Quadrupole microelectrodes sensor implemented with a microfluidic channel in BiCMOS; (**b**) Scanning Electron Microscopy (SEM) picture of a quadrupole sensor.

The experimental setup for the crossover frequency measurement is shown in Figure 5. Once the cells were suspended in the DEP medium, the Eppendorf was linked to the UHF-DEP lab-on-chip thanks to capillary tubes. The cell suspension is injected in the chip by external flow controllers. They apply an input and output pressures in order to regulate the speed and the motion of the cells in the microfluidic channel.

The UHF signal is produced thanks to a radio-frequency signal generator (whose frequency range is adjustable from 10MHz to 1.1 GHz) which is then amplified. The signal generated can reach a magnitude of 10 Vpp while keeping a high purity continuous wave

Preprints (www.preprints.org) | NOT PEER-REVIEWED | Posted: 24 September 2021 doi:10.20944/preprints202109.0424.v1

(CW) signal. During the crossover frequency measurement, the signal voltage is set between 2 and 4 Vpp. The applied signal is then directed to a power divider in order to bias simultaneously with the same signal the pair of thick electrodes, while the thin electrodes are grounded. The DEP signal is propagated until the quadrupole sensor thanks to 50 Ω microstrip transmission lines which are connected to RF probes. The switch driver allows switching between the high frequency applied signal to low frequency applied signal. To measure the first crossover frequency f_{x01}, a low frequency signal can be generated by a second generator whose frequency range can be set from 1 µHz to 80 MHz. Then, the low frequency applied signal is set between 2 and 4 Vpp and propagated through the power divider to the RF probes.

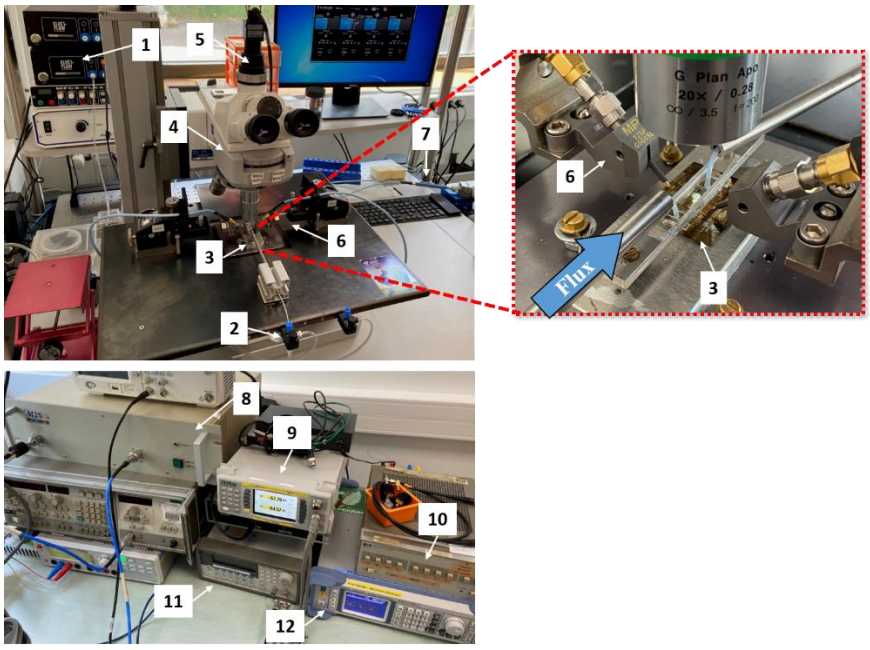

Figure 5. Experimental bench where the crossover frequencies measurements are performed. The labeled parts refer to: (**1**) external flow controllers Elveflow OB1; (**2**) cell suspension; (**3**) UHF-DEP microfluidic chip, a zoomed picture is shown in the red dotted box; (**4**) Scope.A1 Zeiss Microscope; (**5**) camera Axiocam 105 color Zeiss; (**6**) RF probes MPI TITAN T26P-GSG-150; (**7**) power divider; (**8**) power amplifier Bonn Elecktrik BLWA 100-5M ; (**9**) power meter Anritsu ML2496A; (**10**) attenuator/switch driver 11713A HP; (**11**) low frequency generator Agilent 33250A; (**12**) RF signal generator SMB 100A from Rhode & Schwarz.

2.5.2. f_{x01} and f_{x02} crossover frequencies measurements

The aim of this article is to show that we can take benefit from the second crossover frequency f_{x02} to discriminate differentiated cells from undifferentiated cells in GBM cell line and patient GBM cells from primary culture whereas f_{x01} cannot emphasize this discrimination. To do so, we used our lab-on-chip to measure the crossover frequencies and to characterize cells DEP signature according to their different culture conditions (normal medium NM and define medium DM). First, the cells are brought to the characterization area, i.e. the quadrupole sensor, thanks to the external flow controllers. Once a single cell is present in the center of the quadrupole such as in the first picture of Figure 6b, the flow is temporarily cut off and stabilized in order to proceed to the crossover frequency measurement.

Then, the electromagnetic signal is switched on. The Figure 6a shows the quadrupole biased whatever the investigated frequency from low to high frequency range. One can notice that the areas of strong electric field intensity (in orange/red) are located at the different edges of the electrodes. As said before, these zones are related to the pDEP cell behavior. Whereas the area of weak field intensity (in dark blue) is located at the center of

Preprints (www.preprints.org) | NOT PEER-REVIEWED | Posted: 24 September 2021 doi:10.20944/preprints202109.0424.v1

the electrodes, which is assimilated to the nDEP cell behavior. The DEP sensor is biased firstly with the UHF generated signal at 500 MHz. At this frequency range (Figure 3a), we expect the cell to present a nDEP behavior, and it is far from its crossover frequency. The dielectrophoretic force is thus repulsive and the cell is trapped within the central electrical cage created by the quadrupole, as shown in the first picture of Figure 6b. When the flow is stopped, the cell is only submitted to the dielectrophoretic force and the natural gravity. Then, we decrease the frequency of the applied signal. The DEP force starts to become attractive and we can observe a first movement of the cell (second picture in Figure 6b). Finally, the cell is pulled toward the edge of one of the lateral electrodes, which is the pDEP area (last picture in Figure 6b). Hence, we can tune the frequency of the signal from a repulsive state in the center of the sensor to an attractive state. The crossover frequency f_{x02} can be determined from the motion of the cell from the nDEP behaviour to the pDEP behaviour, which can be observed optically under a microscope. In order to precisely identify f_{x02}, we first decrease the frequency of the applied signal by steps of 10 MHz in order to approach the crossover frequency. Then, we slowly scan the frequency by steps of 1 MHz to observe the cell motion. This operation is repeated once again in order to accurately determine f_{x02}. Then, we increase the applied frequency to place the cell in the center of the quadrupole. We turn off the UHF signal generator, and use the switch driver in order to inject the low frequency signal in the lab-on-a-chip and to determine the first crossover frequency f_{x01} of the same cell. The same procedure for the characterization of f_{x02} is used for the measurement of f_{x01}. We turn on the generator and we apply a sinusoidal signal at 10 kHz in order to place the cell in its nDEP behavior. And, we increase the frequency by steps of 10 kHz until observing the cell motion. Then, we scan slowly the frequency by steps of 1 kHz to have an accurate value of the crossover frequency. This characterization process is duplicated to confirm the measured value. Finally, the electric signal is turned off and the flow pressure at the chip inlet is increased to release the characterized cell and renew the cell suspension in the microfluidic channel. A new cell is next trapped and fully characterized following the same method.

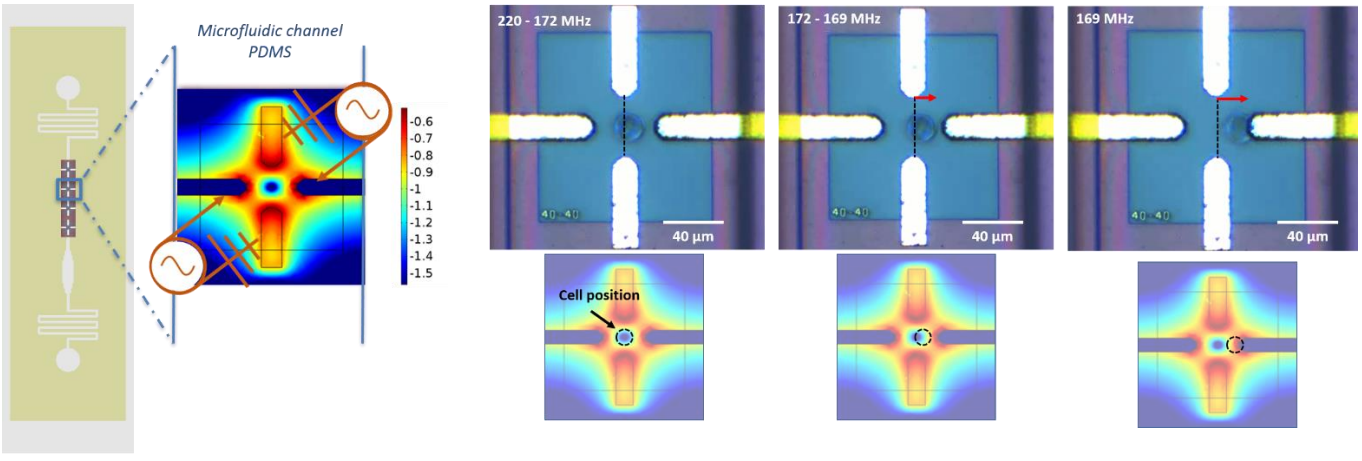

(**a**) (**b**)

Figure 6. Principle of the crossover frequency measurement: (**a**) schematic of the microfluidic chip with a zoom in on one quadrupole sensor. Computation of the biased sensor in a non-uniform electric field (COMSOL Multiphysics®). The scale color corresponds to the normalized electromagnetic field intensity; (**b**) dielectrophoretic response of a single U87-MG NM cell under an UHF applied signal for frequencies between 220 and 169 MHz. The second crossover frequency f_{x02} is measured at 169 MHz.

Hence, the resolution of the two measured crossover frequencies f_{x01} and f_{x02} is respectively 1 kHz and 1 MHz. One should notice that due to the natural biological heterogeneity occurring among a cell population, the crossover frequencies might spread out on a more or less large frequency range. Nevertheless, the repeatability and reproducibility of

Preprints (www.preprints.org) | NOT PEER-REVIEWED | Posted: 24 September 2021 doi:10.20944/preprints202109.0424.v1

the crossover frequency measurements allow to consolidate the collected data. Afterwards, the comparison of different crossover frequencies recorded from distinct cells or conditions is validated with statistical analyses. Hence, we consider that the identification of the DEP signature (collection of crossover frequencies from distinct tumor cells) is representative of the whole cell population.

2.6. Statistical Analysis

Statistical analysis was performed using PAST software. Comparisons between groups were analyzed by ANOVA test. $p < 0.005$ was considered significant (*$p < 0.05$; **$p < 0.01$; ***$p < 0.001$)

3. Results

3.1. Enrichment of CSC in the define medium

In order to enrich the tumor cell populations in undifferentiated cells related to CSC, we cultured U87-MG cells in define medium during 5 days. Morphological changes are observed macroscopically in this stringent culture conditions. As expected, the morphology of U87-MG NM vs U87-MG DM is completely different (Figure 7a). In normal medium, cells are spread out in the petri dish, whereas in define medium, cells develop the ability to form gliomaspheres. It is known that neural stem cells cultured *in vitro* have the capability to generate clonal structures called "neurospheres" [25]. However, just before the DEP characterization, cells are suspended in the DEP medium and gliomaspheres are mechanically broken with the action of a micropipette. When the cell suspension is injected in the lab-on-a-chip, the cells cultured in the different conditions present both a round shape, and no significant difference in morphology can be observed under a microscope (Figure 7b).

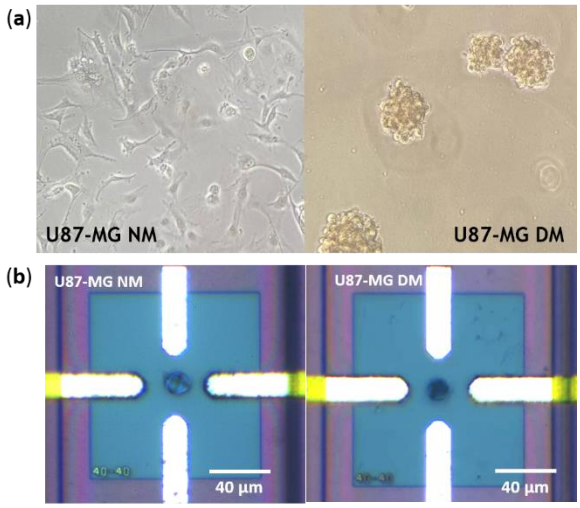

Figure 7. (**a**) Microscope view of the U87-MG cell line cultured in two different conditions: normal medium (NM) and after 2 days in define medium (DM); (**b**) Microscope view of characterized U87-MG cell line trapped in our quadrupole sensor.

To confirm the enrichment of cancer stem cells from total cell population, we achieve a transcriptomic analysis in order to assess the changes of mRNA expression levels related to CSC biomarkers (CD133, Nanog, Sox2 and Oct4) when U87-MG cells were cultured

Preprints (www.preprints.org) | NOT PEER-REVIEWED | Posted: 24 September 2021 doi:10.20944/preprints202109.0424.v1

either in the normal medium or in define medium. mRNA relative quantification of U87-MG cultured in define medium were normalized respectively to the gene expression of U87-MG culture in the normal medium (dotted line) (Figure 8). As expected, CSC transcripts were overexpressed in define medium cultured cells, confirming the enrichment of CSC markers in cell subpopulation.

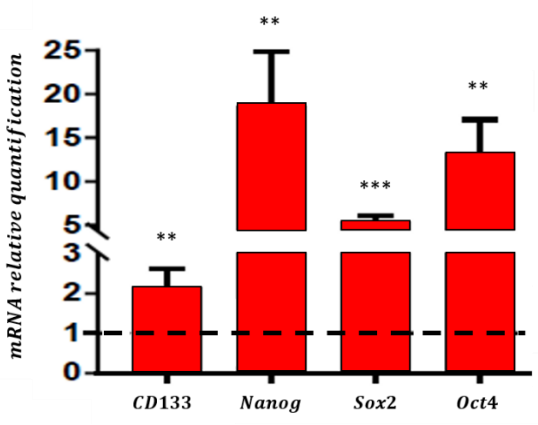

Figure 8. Comparative analysis of gene expression of four undifferentiated markers: CD133, Nanog, Sox2 and Oct4 among U87-MG cell line, cultured in normal medium (dotted line), or in define medium, measured by Real Time PCR. *** represents p-value < 0.001, ** represents p-value < 0.01

3.2. Dielectrophoretic signatures fx01 and fx02 of U87-MG cell line

The U87-MG cell line has been characterized using the microfluidic lab-on-a-chip using the method previously described. The first crossover frequency f_{x01} and the second crossover frequency f_{x02} of the same trapped cells have been successively measured.

The measurement results for both culture conditions are summarized in the violin plot thereby illustrate the distribution over frequency of the data (Figure 9). Violin plots are very similar to box plots, except that they additionally show the probability density curve of the different data. The small white dot marker labels the median value of the dataset (small white dot). Moreover, as for box plot, the first and fourth quartiles of the dataset are represented by the thin black line, and 50% of the whole cell population is concentrated in the thick black line. The extreme peaks correspond to the minimum and maximum values. In Figure 9, one should notice that the scales for the two crossover frequencies are the same except that the unit are kHz and MHz for f_{x01} and f_{x02}, respectively.

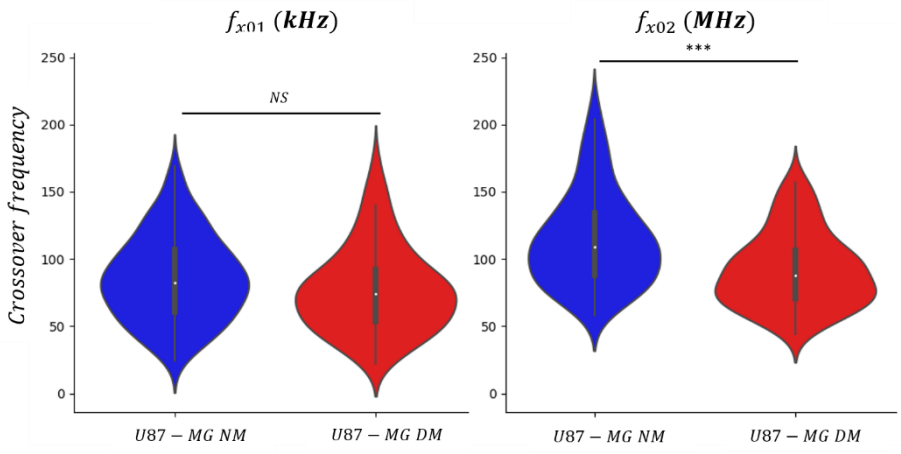

Figure 9. Graphic violin plot representation of U87-MG cells crossover frequencies f_{x01} (left graph) and f_{x02} (right graph), cultured in two different conditions: normal medium (NM) and define medium (DM). *** represents p-value < 0.0001.

Preprints (www.preprints.org) | NOT PEER-REVIEWED | Posted: 24 September 2021 doi:10.20944/preprints202109.0424.v1

Descriptive statistics including cells number, median value and standard deviation of crossover frequency are reported in the Table 2, for distinct culture conditions. One can notice, for both crossover frequencies datasets on Figure 9, the wide-ranging dispersion of measured values, which is also reflected in the value of the standard deviation. This observation is due to the normal heterogeneity of the cell among the GBM cell population. At low frequency, f_{x01} is influenced by the small difference of the cell size and morphology within the cell culture, while at high frequency, f_{x02} might be dependent of intracellular changes or alterations. For instance, during the cell cycle, the nucleus-cytoplasm ratio might differ from a cell to another as they are not synchronized during the culture [26]. However, the violin plot highlights the fact that cell's crossover frequencies are gathered around their respective median value.

Table 2. Values regarding the crossover frequency measurements of the U87-MG cell line.

Cell culture conditions	Crossover frequency	Number of cells measured	Median value	SD
Normal medium (NN)	f_{x01}	139	82 kHz	31.5 kHz
Define medium (DN)		134	74 kHz	32.1 kHz
Normal medium (NN)	f_{x02}	139	109 MHz	35.2 MHz
Define medium (DN)		134	88 MHz	27.9 MHz

A representative number of cells have been individually characterized to statistically consolidate the collected dataset and make significant the established signatures. One can notice that the distribution of the first crossover frequency f_{x01} is mostly the same for the two culture conditions NM vs DM. The median value of f_{x01} for the undifferentiated enriched population (DM) shows no significant difference with the normal conditions: respectively 74 kHz and 82 kHz. Indeed, as shown previously in Figure 8, both U87-MG NM and U87-MG DM presents the same round shape morphology. To the contrary, the distribution of the second crossover frequency f_{x02} exhibits a significant difference despite an overlap in frequency. This can be explained by the fact that GBM cell population cultured in normal condition include a large number of differentiated cells but also few undifferentiated cells. However, for the define condition, the cell population is more concentrated with undifferentiated cells, since presenting stringent survival conditions, the DM medium is more selective than the NM one. Thus, we can observe a decrease of the crossover frequency f_{x02} with the presence of the DM cell pool. The median values for U87-MG NM and U87-MG DM are respectively 109 MHz and 88 MHz. The decrease of f_{x02} shows a significance difference between the two cell population phenotypes, as the p-value is lower than 10^{-3}.

This demonstrates that the undifferentiated cells enriched populations compared to differentiated cells own different intracellular dielectric properties. Despite displaying two crossover frequencies, only the one in the UHF range, f_{x02}, is sufficiently meaningful to be exploited for identifying cells presenting an undifferentiated state or a stemness-like phenotype. These results show how promising UHF-DEP cell profile analysis might be for the discrimination of cell subpopulation within the tumor. Then, we will focus on the second crossover frequency f_{x02} and strengthen the relevance of using UHF-DEP as a discriminant parameter through a kinetic study of the evolution of the stemness phenotype.

3.3. Kinetic evolution of the stemness phenotype

As the enrichment of this cell population is accomplished by seeding normal U87-MG cells in the define medium, either cells already exerting an undifferentiated profile can survive, either other cells must acquire specific features related to stem cells to survive in the define medium. With the acquirement of cell undifferentiated status, cell aggressiveness is increased corresponds to a gain of tumor aggressiveness. The undifferentiation phenomenon is a process that requires several cycles of cell division and we propose to

Preprints (www.preprints.org) | NOT PEER-REVIEWED | Posted: 24 September 2021 doi:10.20944/preprints202109.0424.v1

follow its kinetic by UHF-DEP to demonstrate the potential of the UHF-DEP microsystem developed.

To do so, the U87-MG cell line was cultured within three different conditions: (i) 6 days in normal medium (NM), (ii) 5 days in define medium (DM), (iii) maintained during 21 days in define medium (DM+). The results of the measured crossover frequency f_{x02} are presented in the violin plot chart in Figure 10. In addition to the data already collected previously for U87-MG NM and U87-MG DM cells, we measured again about hundred more crossover frequencies f_{x02} in order to consolidate the obtained DEP signatures and to improve the statistical strength of our analysis.

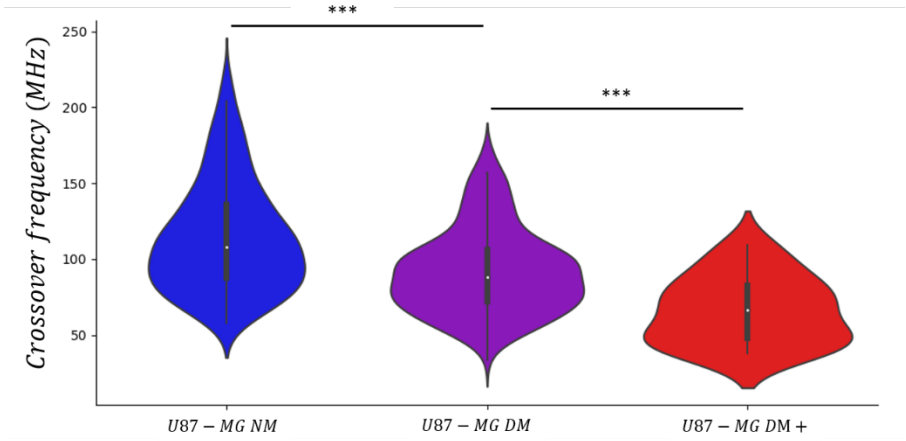

Figure 10. Graphic violin plot representation of U87-MG cells crossover frequency f_{x02}, cultured in three different conditions: (i) 5 days in normal medium (NM), (ii) 5 days in define medium (DM), (iii) 21 days in define medium (DM+). *** represents p-value < 0.001.

Statistics results related to the collected data are reported in Table 3, including the median value and the standard deviation of f_{x02}. As said before, the distribution of the second crossover frequency values is dispersed. This observation is highlighted by the high values of the standard deviation. However, the standard deviation seems to decrease the more the cells are maintained in the define medium. Indeed, as GBM cell line presents a high biological heterogeneity, the define medium tends to select only cells which are able to survive under such stringent culture conditions, i.e. cells with an undifferentiated phenotype. Despite the data dispersion, the violin plot shows that the cell's crossover frequencies values are mostly gathered around their respective median value.

Table 3. Values regarding the crossover frequency measurements of the U87-MG cell line.

Culture condition	Median value	SD
Normal medium (NM)	108 MHz	36.2 MHz
Define medium (DM)	88 MHz	27.9 MHz
Define medium (DM+)	67 MHz	22.1 MHz

In normal medium, the median value of the second crossover frequency is 108 MHz, after 5 days spent in the define medium, the DEP signature decreases to 88 MHz and after 16 additional days spent in define medium, the DEP signature is 67 MHz. The two successive decreases of f_{x02} observed between the three cell population phenotypes present significant differences, as the p-value is lower than 10^{-3}. In correlation with the previous experimentation, a lower dielectric signature seems to potentially characterize cell presenting a stemness-like phenotype.

One can also notice that although more cells were characterized in the NM and DM conditions for this measurement campaign, the median value of the crossover frequency is not affected and remains the same compared to the first campaign (related in Table 2).

 doi:10.20944/preprints202109.0424.v1

It shows the robustness and the reproducibility our method to measure the DEP signatures of cells.

These two experiments demonstrate the ability of the developed UHF-DEP lab-on-chip, to successfully extract information about the potential stemness status of U87-MG cell by the measurement of the second crossover frequency f_{x02}.

3.4. Dielectrophoretic signatures fx01 and fx02 of GBM primary cultures

We measured previously (in section 3.2) the low and high frequency DEP signatures of the U87-MG cell line, cultured in two different conditions in order to induce an undifferentiation corresponding to the CSC subpopulation. From the obtained crossover frequency, f_{x01} did not show any difference between the normal medium and the define medium. However, we demonstrated that f_{x02} presents a significant difference and can be a relevant discriminant parameter to identify the CSC subpopulation. These results of the DEP signatures were obtained from *in vitro* cell line.

To go further, we proposed in the last section of this paper to repeat this experiment on ex-vivo GBM primary culture to demonstrate the potential clinical applications of our approach.

So, the two crossover frequencies f_{x01} and f_{x02} were respectively characterized in GBM primary culture cells derived from 4 patients. These cells were collected after surgery on patients suffering from glioblastoma. Once extracted from the tumor samples, cells were put in culture according to the procedure indicated in Materials and Methods. As for the U87-MG cell line, few minutes before DEP characterization, the *ex vivo* GBM cell were suspended in the DEP medium. Then, for each investigated cell, their two crossover frequencies f_{x01} and f_{x02} were measured with the previously described protocol.

Before DEP characterizations, the GBM cell population was first separated into two subpopulations: CD133- and CD133+. CD133 is a transmembrane protein expressed in human hematopoietic stem cells and progenitor cells [27]. As said before, CD133 is a biomarker associated with stem cells, tumor and regeneration. It is possible to mark cell with monoclonal antibodies anti-AC133 coupled with a fluorochrome to detect the presence of the peptide CD133 on cell surface [28]. Nevertheless, CD133 can be also expressed in differentiated cancer cells, so the whole cell population will present a fluorescent intensity gradient [29]. Hence, we impose a threshold of the fluorescent intensity during the passage of the cells in the flow cytometer in order to define the two subpopulations. The CD133+ population is the cell population that overexpresses the marker and thus, is enriched of CSC, while the CD133- population is the differentiated cancer cells [27]. Therefore, we separate and isolate the enriched CSC glioblastoma cell population from differentiated tumor cell thanks to a fluorescent marker, before DEP characterizations of these two populations. The results of the measured crossover frequencies f_{x01} and f_{x02} for the both populations are presented in the violin plot (Figure 11).

Preprints (www.preprints.org) | NOT PEER-REVIEWED | Posted: 24 September 2021 doi:10.20944/preprints202109.0424.v1

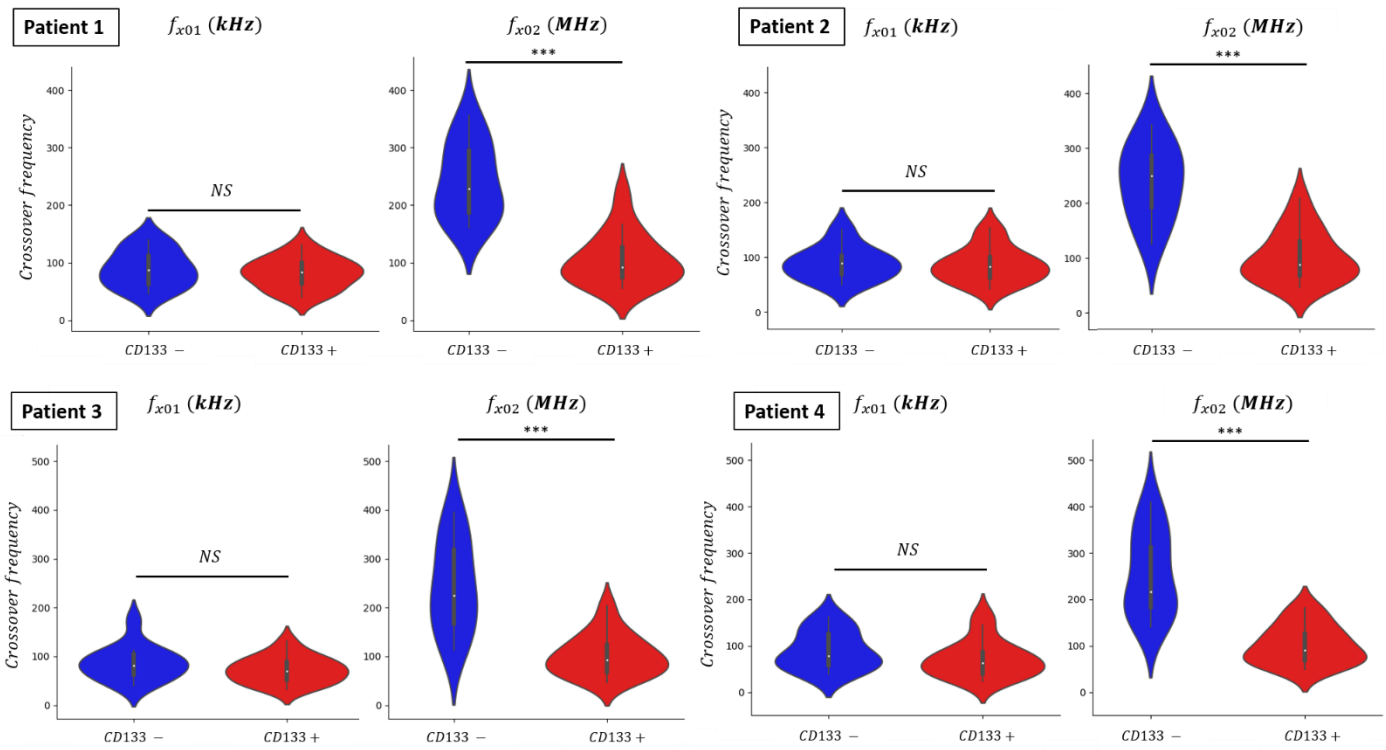

Figure 11. Graphic violin plot representation of crossover frequencies f_{x01} and f_{x02} of GBM primary cells collected from four different patients. *** represents p-value < 0.001.

One should notice that the scale for the two crossover frequencies is the same except that the unit are kHz and MHz for respectively f_{x01} and f_{x02}. The data distribution of crossover frequencies f_{x01} and f_{x02} from the characterized glioblastoma cell shows similar violin plot shapes although cells derived from four different patients (Figure 11). Indeed, we can expect from *ex vivo* GBM cells to be even more genetically heterogeneous from a patient to another than immortalized U87-MG cell line. Median values of the crossover frequencies measured for each isolated population are reported in the Table 4. The obtained results highlight that our DEP cell analyzer lab-on-chip is a relevant and reliable tool to study and analyze either *in vitro* or *ex vivo* dissociated samples.

Table 4. Values of the crossover frequency measurements of the GBM primary culture extracted from tumor samples of four different patients.

	Cell population	Crossover frequency	Median value
Patient 1	CD133 -	f_{x01}	88 kHz
	CD133 +		83 kHz
	CD133 -	f_{x02}	229 MHz
	CD133 +		92 MHz
Patient 2	CD133 -	f_{x01}	89 kHz
	CD133 +		83 kHz
	CD133 -	f_{x02}	248 MHz
	CD133 +		86 MHz
Patient 3	CD133 -	f_{x01}	81 kHz
	CD133 +		70 kHz
	CD133 -	f_{x02}	225 MHz
	CD133 +		92 MHz
Patient 4	CD133 -	f_{x01}	78 kHz
	CD133 +		63 kHz
	CD133 -	f_{x02}	216 MHz

 doi:10.20944/preprints202109.0424.v1

	CD133 +	91 MHz

The distribution of the first crossover frequency f_{x01} is mostly the same for the two isolated population CD133- vs CD133+. The median value of f_{x01} for the undifferentiated enriched population (CD133+) shows no significant change with the differentiated population. At low frequency, the largest signature dissimilarity between the two conditions corresponds to the patient 4 where f_{x01} displays a change of 15 kHz between CD133- and CD133+ conditions. However, this difference is not statistically significant to discriminate the subpopulation of CSC overrepresented in the CD133+ cell population. The distribution of the second crossover frequency f_{x02} exhibits a difference despite the overlap among the measured values. This can be explained by the method by which CSCs cell population have been enriched through flow cytometry. Indeed, the CD133 biomarker is not a binary label as the whole cell population might present a more or less fluorescent intensity. With this fluorescent gradient, we choose a threshold to separate GBM cells into two subpopulations and to be selective toward CSC population. Thus, we can observe a decrease of the crossover frequency f_{x02} with the presence of the CD133+ cell pool. The median values of the second crossover frequency display the smallest change for the patient 4 which is 125 MHz. The decrease of f_{x02} shows a significant difference, as the p-value is lower than 10^{-3}, between the two cell population phenotypes. Moreover, one can notice on the Figure 11 that at high frequency, the CD133+ cell population displays a stoutness around the median value compare to the distribution concerning the CD133- cell population underlying that the crossover frequency values are gathered around their median.

Such results validate that we can exploit the intracellular dielectric properties difference between differentiated and undifferentiated cells by measuring the second crossover frequency f_{x02}. The cells extracted from patients' GBM tumor samples show similar behavior as observed with *in vitro* GBM cell line. Even if the *ex vivo* cell median values of f_{x02} are not the same as the *in vitro* results, we can extrapolate that if in an *ex vivo* cell hold a low second crossover frequency values, it means that it should potentially present a stemness phenotype.

4. Conclusion

Along this article, we used an innovative microfluidic device based on high frequency dielectrophoresis for single-cell characterization in order to discriminate and identify the cancer stem cell subpopulation. First, we evaluated the discrimination capabilities of our microfluidic device *in vitro* on glioblastoma cell line. U87-MG cells were cultured in two distinct conditions: one inducing a differentiation and the second selecting immature and undifferentiated cells. Our results suggest that the expression of biological CSC markers and the measurement of the UHF crossover frequency f_{x02} are closely linked. At this frequency range, our lab-on-chip is able to interact with the intracellular content, which is more representative of the cell undifferentiated biologic features making UHF-DEP greatly relevant to investigate the stemness status of cancer cells. As a first step towards clinical experiments, some GBM cells were extracted and cultured from patient's tumors. These GBM primary cells have been sorted in two subpopulations according to their expression level of CSC biomarker CD133. Whatever the considered patient, observed DEP signatures display the same profile. As previously identified, f_{x02} shows a more significant and more important difference between the two cell phenotypes than f_{x01} and so is confirmed to be a relevant CSC discriminant parameter. As primary culture cells are more representative of tumor than cell lines, we believe that it might be possible to transpose this capability of UHF-DEP cell characterization for recognizing "stemness" features from tumor cells derived to a broad range of GBM patients.

UHF-DEP is a very promising tool with the great potential to discriminate cell according to their internal biological properties. Hence, from the identification of UHF-DEP signatures, we can see the perspective to develop a cell sorting device for isolating cancer stem cells [30]. In the future, the early detection of CSC subpopulation in glioma tumor

with UHF-DEP approach could have a prognosis value on therapeutic response and might allow to adapt therapeutic strategy following diagnosis.

Author Contributions: Conceptualization, E.L. and E.B.; methodology, R.M. and S.S.; software, E.L. and E.B.; formal analysis, E.L and R.M; investigation, E.L. and E.B.; data curation, A.P.; writing—original draft preparation, E.L. and E.B.; writing—review and editing, A.P. and F.L.; supervision, C.D. and B.B.; project administration, A.P. and F.L.; funding acquisition, A.P. and F.L. All authors have read and agreed to the published version of the manuscript.

Funding: This research was funded by the European Union's Horizon 2020 research and innovation program under grant number 737164, and by the Nouvelle Aquitaine Council with the Oncosometrack project and by funds from the Pediatric Research Institute Foundation (IRP 18/06). F.M. was supported by a fellowship from the Italian Association for Cancer Research (AIRC) (ID 19575). E.P. was supported by a fellowship from the Umberto Veronesi Foundation (#1142).

Institutional Review Board Statement: The study was conducted according to the guidelines of the Declaration of Helsinki, and approved by the committee of the Sperimentazione Clinic of Padova Provincia (n°2462P, the 29th November 2016).

Informed Consent Statement: Informed consent was obtained from all subjects involved in the study as described in the Materials and Methods paragraph.

Acknowledgments: We are grateful to Dr. Chiara Frasson (Pediatric Research Institute, Padova, Italy) for technical assistance in flow cytometry procedures.

Conflicts of Interest: The authors declare no conflict of interest.

References

1. Cheray, M.; Bégaud, G.; Deluche, E.; Nivet, A.; Battu, S.; Lalloué, F.; Verdier, M.; Bessette, B. Cancer Stem-Like Cells in Glioblastoma. *Exon Publications* **2017**, 59–71, doi:10.15586/codon.glioblastoma.2017.ch4.
2. Goldsmith, H.S. Potential Improvement of Survival Statistics for Glioblastoma Multiforme (WHO IV). *Surg Neurol Int* **2019**, *10*, 123, doi:10.25259/SNI-185-2019.
3. Stupp, R.; Mason, W.P.; van den Bent, M.J.; Weller, M.; Fisher, B.; Taphoorn, M.J.B.; Belanger, K.; Brandes, A.A.; Marosi, C.; Bogdahn, U.; et al. Radiotherapy plus Concomitant and Adjuvant Temozolomide for Glioblastoma. *New England Journal of Medicine* **2005**, *352*, 987–996, doi:10.1056/NEJMoa043330.
4. Tabatabai, G.; Weller, M. Glioblastoma Stem Cells. *Cell Tissue Res* **2011**, *343*, 459–465, doi:10.1007/s00441-010-1123-0.
5. Gossett, D.R.; Weaver, W.M.; Mach, A.J.; Hur, S.C.; Tse, H.T.K.; Lee, W.; Amini, H.; Di Carlo, D. Label-Free Cell Separation and Sorting in Microfluidic Systems. *Anal Bioanal Chem* **2010**, *397*, 3249–3267, doi:10.1007/s00216-010-3721-9.
6. R. Pethig, Dielectrophoresis: Theory, Methodology and Biological Applications, First published: 25 March 2017, Print ISBN:9781118671450 |Online ISBN: 9781118671443, |doi:10.1002/9781118671443 Copyright © 2017 John Wiley & Sons, Ltd. All rights reserved
7. Cottet, J.; Fabregue, O.; Berger, C.; Buret, F.; Renaud, P.; Frénéa-Robin, M. MyDEP: A New Computational Tool for Dielectric Modeling of Particles and Cells. *Biophysical Journal* **2019**, *116*, 12–18, doi:10.1016/j.bpj.2018.11.021.
8. Afshar, S.; Fazelkhah, A.; Braasch, K.; Salimi, E.; Butler, M.; Thomson, D.; Bridges, G. Full Beta-Dispersion Region Dielectric Spectra and Dielectric Models of Viable and Non-Viable CHO Cells. *IEEE Journal of Electromagnetics, RF and Microwaves in Medicine and Biology* **2020**, 1–1, doi:10.1109/JERM.2020.3014062.
9. Fazelkhah, A.; Afshar, S.; Braasch, K.; Butler, M.; Salimi, E.; Bridges, G.; Thomson, D. Cytoplasmic Conductivity as a Marker for Bioprocess Monitoring: Study of Chinese Hamster Ovary Cells under Nutrient Deprivation and Reintroduction. *Biotechnology and Bioengineering* **2019**, *116*, 2896–2905, doi:10.1002/bit.27115.

10. Cottet, J.; Fabregue, O.; Berger, C.; Buret, F.; Renaud, P.; Frénéa-Robin, M. *MyDEP: A New Computational Tool for Dielectric Modeling of Particles and Cells*; Zenodo, 2019, doi: 10.5281/zenodo.1321928.
11. Pethig, R.; Menachery, A.; Pells, S.; De Sousa, P. Dielectrophoresis: A Review of Applications for Stem Cell Research, *Journal of Biomedicine and Biotechnology*, **2010**, doi:10.1155/2010/182581
12. Sato, N.; Yao, J.; Sugawara, M.; Takei, M. Numerical Study of Particle-Fluid Flow Under AC Electrokinetics in Electrode-Multilayered Microfluidic Device. *IEEE Transactions on Biomedical Engineering* **2019**, *66*, 453–463, doi:10.1109/TBME.2018.2849004.
13. Du, X.; Ma, X.; Li, H.; Li, L.; Cheng, X.; Hwang, J.C.M. Validation of Clausius–Mossotti Function in Wideband Single-Cell Dielectrophoresis. *IEEE Journal of Electromagnetics, RF and Microwaves in Medicine and Biology* **2019**, *3*, 127–133, doi:10.1109/JERM.2019.2894100.
14. Alazzam, A.; Stiharu, I.; Bhat, R.; Meguerditchian, A.-N. Interdigitated Comb-like Electrodes for Continuous Separation of Malignant Cells from Blood Using Dielectrophoresis. *ELECTROPHORESIS* **2011**, *32*, 1327–1336, doi:10.1002/elps.201000625.
15. Choi, S.; Park, J.-K. Microfluidic System for Dielectrophoretic Separation Based on a Trapezoidal Electrode Array. *Lab on a Chip* **2005**, *5*, 1161–1167, doi:10.1039/B505088J.
16. Vahey, M.D.; Voldman, J. An Equilibrium Method for Continuous-Flow Cell Sorting Using Dielectrophoresis. *Anal. Chem.* **2008**, *80*, 3135–3143, doi:10.1021/ac7020568.
17. Chung, C.; Pethig, R.; Smith, S.; Waterfall, M. Intracellular Potassium under Osmotic Stress Determines the Dielectrophoresis Cross-over Frequency of Murine Myeloma Cells in the MHz Range. *ELECTROPHORESIS* **2018**, *39*, 989–997, doi:10.1002/elps.201700433.
18. Chung, C.; Waterfall, M.; Pells, S.; Menachery, A.; Smith, S.; Pethig, R. Dielectrophoretic Characterisation of Mammalian Cells above 100 MHz. **2011**, 9, doi:10.5617/jeb.196.
19. Manczak, R.; Saada, S.; Tanori, M.; Casciati, A.; Dalmay, C.; Bessette, B.; Begaud, G.; Battu, S.; Blondy, P.; Jauberteau, M.O.; et al. High-Frequency Dielectrophoresis Characterization of Differentiated vs Undifferentiated Medulloblastoma Cells. *2018 EMF-Med 1st World Conference on Biomedical Applications of Electromagnetic Fields (EMF-Med)* **2018**, 1–2, doi:10.23919/emf-med.2018.8526006.
20. Casciati, A.; Tanori, M.; Manczak, R.; Saada, S.; Tanno, B.; Giardullo, P.; Porcù, E.; Rampazzo, E.; Persano, L.; Viola, G. Human Medulloblastoma Cell Lines: Investigating on Cancer Stem Cell-like Phenotype. *Cancers* **2020**, *12*, 226, doi : 10.3390/cancers12010226
21. Pistollato, F.; Persano, L.; Puppa, A.D.; Rampazzo, E.; Basso, G. Isolation and Expansion of Regionally Defined Human Glioblastoma Cells In Vitro. *Current Protocols in Stem Cell Biology* **2011**, *17*, 3.4.1-3.4.10, doi:10.1002/9780470151808.sc0304s17.
22. Pistollato, F.; Abbadi, S.; Rampazzo, E.; Persano, L.; Puppa, A.D.; Frasson, C.; Sarto, E.; Scienza, R.; D'avella, D.; Basso, G. Intratumoral Hypoxic Gradient Drives Stem Cells Distribution and MGMT Expression in Glioblastoma. *STEM CELLS* **2010**, *28*, 851–862, doi:10.1002/stem.415.
23. Frasson, C.; Rampazzo, E.; Accordi, B.; Beggio, G.; Pistollato, F.; Basso, G.; Persano, L. Inhibition of PI3K Signalling Selectively Affects Medulloblastoma Cancer Stem Cells. *BioMed Research International* **2015**, *2015*, e973912, doi:10.1155/2015/973912.
24. Hjeij, F.; Dalmay, C.; Bessaudou, A.; Blondy, P.; Pothier, A.; Bessette, B.; Bégaud, G.; Jauberteau, M.O.; Lalloué, F.; Kaynak, C.B.; et al. UHF Dielectrophoretic Handling of Individual Biological Cells Using BiCMOS Microfluidic RF-Sensors. *2016 46th European Microwave Conference (EuMC)* **2016**, 265–268, doi:10.1109/eumc.2016.7824329.
25. Suslov, O.N.; Kukekov, V.G.; Ignatova, T.N.; Steindler, D.A. Neural Stem Cell Heterogeneity Demonstrated by Molecular Phenotyping of Clonal Neurospheres. *PNAS* **2002**, *99*, 14506–14511, doi:10.1073/pnas.212525299.

26. Pethig, R.; Bressler, V.; Carswell-Crumpton, C.; Chen, Y.; Foster-Haje, L.; García-Ojeda, M.E.; Lee, R.S.; Lock, G.M.; Talary, M.S.; Tate, K.M. Dielectrophoretic Studies of the Activation of Human T Lymphocytes Using a Newly Developed Cell Profiling System. *ELECTROPHORESIS* **2002**, *23*, 2057–2063, doi:10.1002/1522-2683(200207)23:13<2057::AID-ELPS2057>3.0.CO;2-X.
27. Li, Z. CD133: A Stem Cell Biomarker and Beyond. *Experimental Hematology & Oncology* **2013**, *2*, 17, doi:10.1186/2162-3619-2-17.
28. Ren, F.; Sheng, W.-Q.; Du, X. CD133: A Cancer Stem Cells Marker, Is Used in Colorectal Cancers. *World J Gastroenterol* **2013**, *19*, 2603–2611, doi:10.3748/wjg.v19.i17.2603.
29. Kemper, K.; Sprick, M.R.; Bree, M. de; Scopelliti, A.; Vermeulen, L.; Hoek, M.; Zeilstra, J.; Pals, S.T.; Mehmet, H.; Stassi, G.; et al. The AC133 Epitope, but Not the CD133 Protein, Is Lost upon Cancer Stem Cell Differentiation. *Cancer Res* **2010**, *70*, 719–729, doi:10.1158/0008-5472.CAN-09-1820.
30. T. Provent *et al.*, "A High Frequency Dielectrophoresis Cytometer for Continuous Flow Biological Cells Refinement," *2020 50th European Microwave Conference (EuMC)*, 2021, pp. 921-924, doi: 10.23919/EuMC48046.2021.9338228.